CALM WATER RESISTANCE AND SELF-PROPULSION SIMULATIONS INCLUDING CAVITATION FOR AN LNG CARRIER IN EXTREME TRIM CONDITIONS

M. Maasch[1], O. Turan[1] and M. Khorasanchi[1], Ivy Fang[2]

[1]Department of Naval Architecture and Marine Engineering, University of Strathclyde, 100 Montrose Street, Glasgow G4 0LZ, UK, matthias.maasch@strath.ac.uk, o.turan@strath.ac.uk, mahdi.khorasanchi@strath.ac.uk
[2]Senior Specialist at Strategic Research and Technology Policy Group Lloyd's Register EMEA, London, UK, ivy.fang@lr.org

ABSTRACT

In recent years many studies and real-life applications dealing with trim optimisation have shown that operating a ship at small trim angles can improve the energy efficiency by up to 5% depending on ship speeds and loading conditions. This efficiency gain mainly results from the re-positioning of underwater hull features, such as the bulbous bow or the stern bulb. Different to the above described approach the present study deals with operating a LNG Carrier at an extreme bow-up trim angle of $\theta = -1.9\,deg$. In order to predict the performance, URANS virtual towing tank simulations in calm water were performed for both, nominal resistance conditions and self-propulsion conditions including cavitation. The numerical results, including the ship resistance, the nominal propeller wake field and the simulation of propeller cavitation in self-propulsion conditions indicated a largely improved performance. Due to a significant reduction in nominal resistance by up to 27.5% the ship self-propulsion point in extreme trim conditions was found at a lower propeller rotation rate compared to level trim conditions. This also reduced the cavitation volume and finally resulted in a delivered power reduction of up to 28.8%.

Keywords: Extreme Trim Operation, Unsteady RANSE, Calm Water Resistance Performance, Automatic Wake Analysis, Self-Propulsion Performance, Cavitation Simulation

1. INTRODUCTION

Out of the many possibilities to improve a vessel's performance with regard to its environmental impact, from a hydrodynamic point of view the main target is reducing the ship resistance along with improving the propeller inflow to ultimately increase the propulsive performance. One of the methods to improve the hydrodynamic performance of ships when under way in off-design conditions is to operate in trim conditions. This practice aims on improving the hydrodynamic performance of certain ship features such as the bulbous bow and the ship stern. For a ship in off-design conditions the bow and stern features are often out of place and can therefore cause additional resistance rather than improving the flow around the hull. (Górski et al., 2013) state that by trimming the ship either to stern or to bow at constant displacement the ship wave making resistance can be improved significantly. Therefore trim optimisation can be a helpful tool to find the best operating point for different speeds, loading conditions (ship displacement) and water depths. (Hansen and Hochkirch, 2013) argue that since there is no single optimum trim value for all operating conditions, trim optimisation is a comprehensive task including experimental model testing and Computational Fluid Dynamic (CFD) simulations for both resistance conditions and self-propulsion conditions. FORCE Technology (Reichel et al., 2014) performed trim model tests for tankers, container vessels, Liquefied Natural Gas Carriers (LNGC), Ro-Ro vessels and ferries (among others) and found that the residual resistance and therefore the wave making resistance can significantly improve from even-keel values. In addition, improvements in the propulsive conditions contribute to the performance change as the propeller inflow can change.

Trim ($trim = T_A - T_F$) is defined as the difference in aft (stern) draft $\mathrm{T_A}$ and forward (bow) draft $\mathrm{T_F}$ resulting from a rotation around a transverse axis pointing through the centre of flotation (COF), assuming constant displacement. The draft is measured at the draft marks at the aft and the bow of the ship, usually located at the respective perpendiculars. This allows calculating the trim angle θ using the ship length between its perpendiculars $\mathrm{L_{PP}}$ by $tan\,\theta = (T_A - T_F)/L_{PP}$. With the draft at the aft ship mark being higher as the draft at the foreship mark the ship is trimmed to the stern and vice versa the ship is trimmed to the bow. (Birbanescu-Biran and Pulido, 2014)

Contrary to the standard trim operation approach this study focuses on pushing the limits of trim further, to significantly reduce the ship underwater surface. This makes the frictional resistance rather than the wave making resistance the optimisation target in the first place.

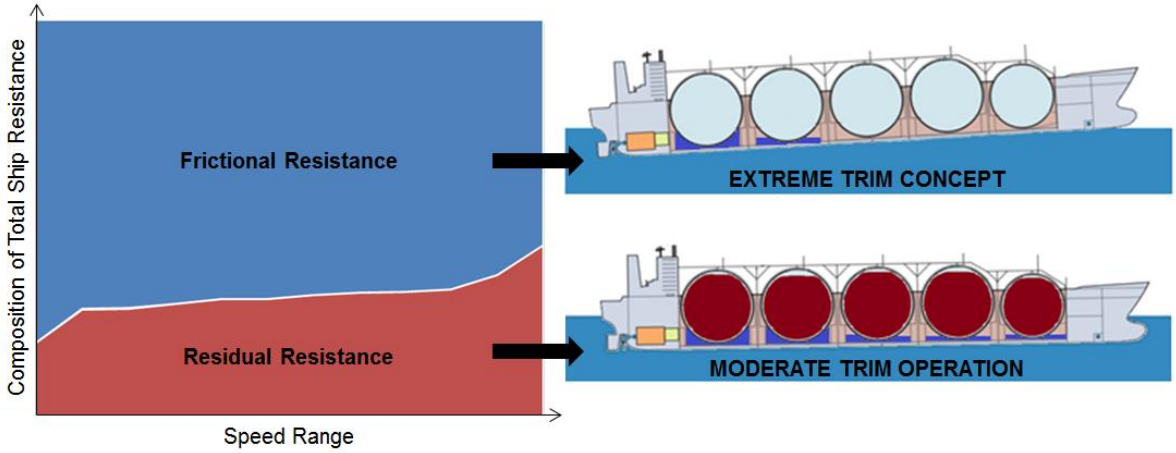

Figure 1 - Composition of Ship Resistance over Ship Speed and relation to different trim operation concepts

As Figure 1 (LHS) indicates the frictional resistance can have a high proportion of the total resistance over a broad range of speeds for a LNGC. Therefore a reduction of the frictional resistance would have a significant effect on the total ship resistance and finally on the propulsive performance, if the propulsive conditions (propeller inflow field) would remain suitable for the working propeller. Extreme trim conditions can only be reasonable if the ship propulsor operates fully submerged. Therefore extreme trim is applied to the stern. The ship displacement has to be reduced as much as possible for operating in extreme conditions. Figure 1 (RHS) shows the concept of the approach and the difference to the standard (moderate) trim operation. Whereas moderate trim operation is often applied in various design and off-design loading conditions, extreme trim operation is applied only in ballast conditions.

The aim of the present study was to analyse the impact of extreme trim on the operational calm water performance of an LNGC by running nominal resistance and self-propulsion CFD simulations over a range of speeds. Both, resistance and the quality of the propeller wake field are suitable to predict the propulsive performance of a ship as with a reduced total hull resistance and a nominal wake field with high uniformity the requirement on the delivered power to the propeller decreases (Ploeg, 2012). An LNGC operates a well-defined trading pattern in which a significant proportion of the operational time is spent in ballast condition. Furthermore, due to its type of loading, this ship type offers a high overall volume of ballast tanks which enables the ship to reach a reasonable draft in transit conditions. This makes an LNGC a suitable target for extreme trim operation.

2. METHODOLOGY

Model-scale CFD simulations were carried out in nominal resistance and self-propulsion conditions for level trim and extreme trim. Three speeds v_1, v_2 and v_3 were covered corresponding to full scale speeds of $14\ knots$, $16\ knots$ and $18\ knots$.

The numerical process was driven by FRIENDSHIP Systems' software tool CAESES. Its in-build software connector was used to couple external software, as shown in Figure 2. Integrated software packages were Bentley's Maxsurf Stability tool and SIEMENS' CFD workbench STAR-CCM+. CAESES' programming environment (i.e. feature definitions) was used to customize the software connections and the CFD pre-processing and post-processing. The details of the study workflow are outlined below following the numbering shown in Figure 2.

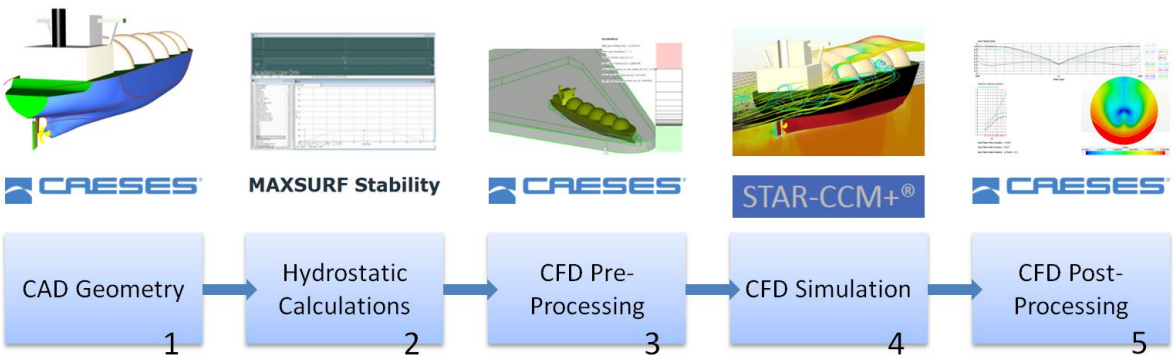

Figure 2 - Study Workflow

(1) A CAD ship hull of a single-screw LNGC was modelled in CAESES (see Figure 3 LHS for 3D-view of LNGC model), resulting in a Panel Mesh geometry to be used in Maxsurf Stability for hydrostatic calculations as well as a watertight STL file to be used in STAR-CCM+ for Virtual Towing Tank simulations. In order to determine the nominal total resistance force similar to towing tank experiments, the ship hull was exported to Maxsurf and STAR-CCM+ without appendages and deck structure. For running the self-propulsion simulations, the complete LNGC with

(2) Maxsurf Stability was used to calculate the hydrostatics of the ship model. By providing a loadcase definition (lightship loading and ballast tank loadings) Maxsurf determined the ship mass and its longitudinal centre of buoyancy (LCB) which was further used as longitudinal centre of gravity (LCG) within the STAR-CCM+ Dynamic Fluid Body Interaction (DFBI) module. Maxsurf also calculated the trim angle, the longitudinal centre of flotation (LCF) and the draft at the LCF.

(3) The hydrostatic results were used to re-position the ship hull in CAESES before generating the numerical mesh in STAR-CCM+. Firstly, the hull was rotated by the trim angle around the LCF and secondly shifted vertically setting the draft at LCF. The benefit of this method is that the DFBI model only had to handle small dynamic motions of the ship body. Hence, the simulation converged to its near-steady state much faster, compared to a simulation where the ship body starts its motion in level trim conditions. In addition, the parametric CAD modeller of CAESES was used to design geometry-dependent mesh refinement regions. Volumes at the bow, the stern and along the hull were designed to place fine mesh cells only in regions where it was necessary (see Figure 3). This approach significantly reduced the overall number of cells in the computational domain compared to a standard domain setup using box shaped refinements while at the same time important flow features, such as the bow and stern flow, were captured accurately. Due to the parametric setup of the CFD pre-processing the numerical mesh automatically adapted to any chances of the hydrostatic floating position of the LNGC before running the simulation. Consequently, the effort of setting up a CFD simulation for different trim angles was reduced to a single-click action as CAESES triggered all coupled software in the chain automatically.

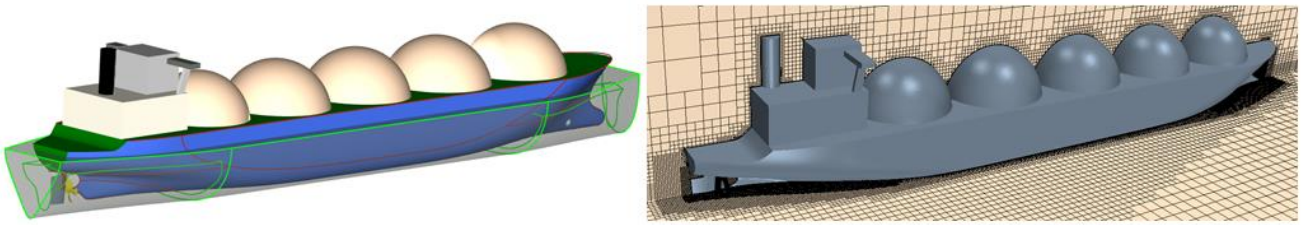

Figure 3 - Refinement volumes at bow, stern and around hull (LHS) for fine mesh regions created in STAR-CCM+ (RHS)

(4) Two types of CFD simulations were carried out using STAR-CCM+. Firstly, the bare LNGC hull was simulated in a VTT over a range of speeds allowing the hull to move freely for pitch and heave motions. Secondly, the full LNGC hull including superstructure and appendages was simulated in a VTT self-propulsion simulation with a fixed hull (no motions allowed) and propeller cavitation. Details of the numerical setup are outlined in the next section. The nominal resistance simulations were evaluated for the total resistance force, its shear and pressure force components and the dynamic motions of the LNGC. Furthermore the nominal wake fields were captured and analysed for each speed. The analysis of the self-propulsion simulations included the recording of the propulsive quantities such as the propeller rotation rate, the delivered power and the cavitation volume.

(5) CAESES was used to evaluate the nominal wake field by reading a csv file holding the axial flow velocity normal to the propeller disc. A custom developed Wake Analysis Tool (WAT) plotted the wake velocity ratio and finally calculated the axial mean wake fraction, the axial mean wake variation and the axial mean wake L2-norm gradient (a definition of the wake gradient can be found in (Ploeg, 2012). Figure 4 presents a snapshot of the graphical output of the WAT showing the axial velocity ratio profiles over the propeller wake angle (top) and the maximum velocity variation, the average velocity ratio and the maximum velocity gradient for each measured propeller wake disc radius. This allowed judging the quality of the wake field in terms of uniformity for the axial velocity component.

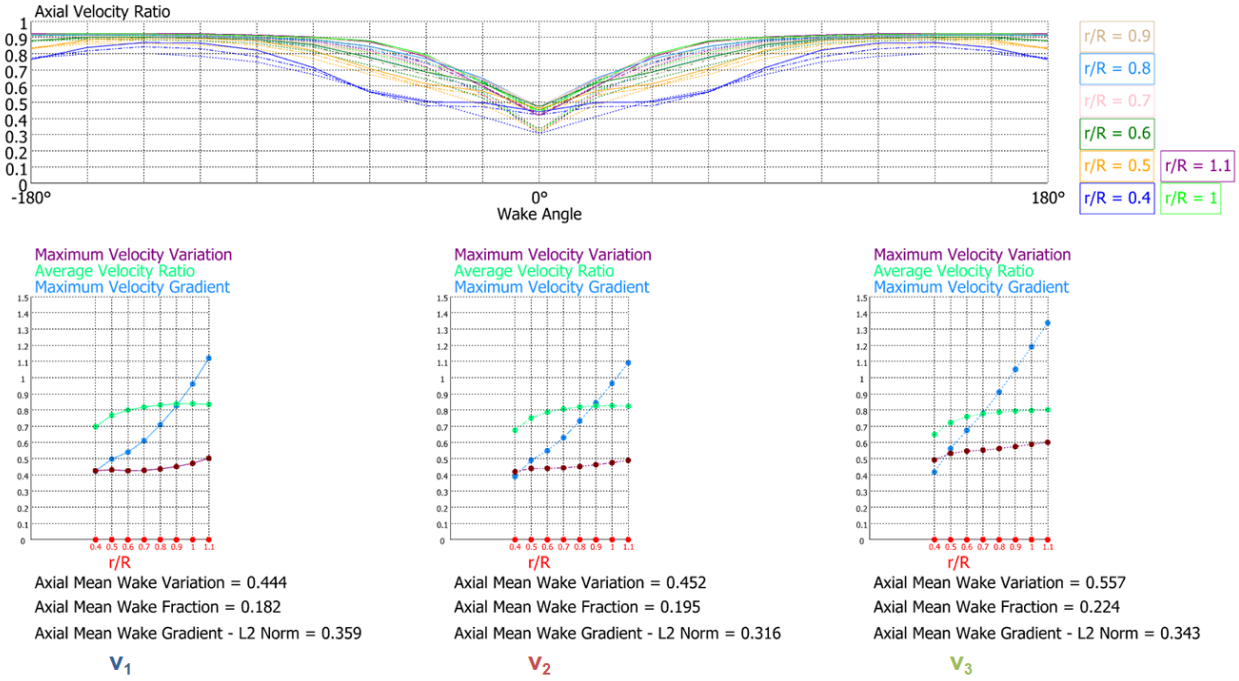

Figure 4 - Sample of graphical output of Wake Analysis Tool (WAT) for extreme trim simulations

Finally, all results were compared between level trim simulations and extreme trim simulations. The nominal resistance results were used to predict a self-propulsion performance trend. This prediction was further compared to the results of the self-propulsion simulations.

3. NUMERICAL SETUP

SIEMENS commercial software STAR-CCM+ was used to carry out marine CFD simulations. For both cases (nominal resistance and self-propulsion simulation setup) the free surface was captured using a Volume of Fluid model (VOF). This model resolved the interface between the two immiscible fluids water and air. Although this model works best on a fine hexahedral numerical mesh it also provides reasonable solutions on relatively coarse meshes if the free surface remains smooth, i.e. no braking waves occur. (SIEMENS, 2017)

The size of the boxed shaped domain with the LNGC in its centre was kept small with only 1.2 ship length in each spatial direction. All Unsteady Reynolds-averaged Navier-Stokes (URANS) simulations employed the two-equation $k-\omega\ SST$ turbulence model that solves the transport equations for the turbulent kinetic energy k and the specific dissipation rate ω. This model is able to switch from the standard $k-\epsilon$ model used to solve the far field flow to the $k-\omega$ model used to solve the near wall flow by blending between the models depending on the wall distance. A detailed turbulence model formulation can be found in (Menter, 1994). In order to reduce the computational effort the near wall flow was modelled aiming high $Y+$ values. Thus, fewer cells inside the boundary layer were necessary. An implicit unsteady first order time model was used. The time step varied for nominal resistance and self-propulsion simulations and will be further described below.

The validity (appropriate near wall solution and numerical stability) of the simulation was judged by monitoring the $Y+$ value on the underwater hull, the Courant-Friedrichs-Lewy number (CFL) on the free surface close to the hull and the solver residuals along with the convergence of the values of interest. As mentioned above, a high $Y+\gg 30$ was aimed so that STAR-CCM+ applied wall-functions. As the flow around the ship decelerates at the stern, a few mesh cells showed smaller values of $Y+<30$, especially near stagnation or separation, which was deemed acceptable (see Figure 5). For the self-propulsion setup $Y+<5$ was aimed for the propeller wall to solve the viscous sublayer.

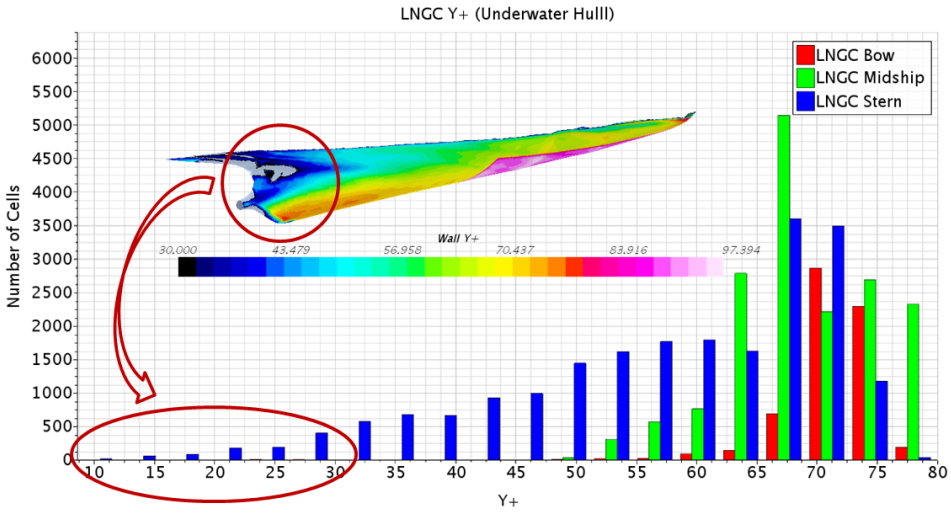

Figure 5 - Y+ on the LNGC underwater hull (nominal resistance simulation at $\mathbf{v_3}$)

The CFL number expresses through how many cells one fluid element travels in one time step. For the highly time-dependent self-propulsion simulations a $CFL \leq 1$ was targeted. For the nominal resistance simulations higher values of $CFL < 20$ were appropriate as the flow field naturally reached a near-steady state. The solver residuals, quantifying the error in the solution of the discretized transport equations, showed mostly good convergence for both nominal and self-propulsion simulations (see Figure 6). With multiple speeds simulated within one nominal resistance simulation, the residuals spiked at each speed change (Figure 6 LHS). Due to the minimal submergence of the propeller the self-propulsion residuals for the volume fraction of air and continuity did not converge well (Figure 6 RHS) as air was sucked down by the rotating propeller (see Figure 14 for propeller ventilation).

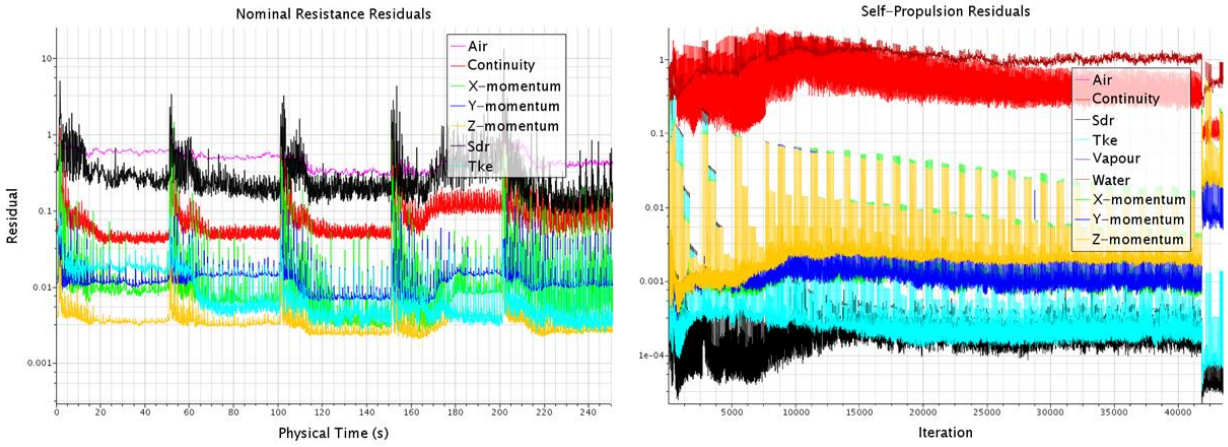

Figure 6 - Solver residuals for nominal resistance simulations (LHS) and self-propulsion simulations (RHS)

Overall the numerical simulation setup was deemed valid and was kept unchanged between the level trim and extreme simulations. Further differences between the nominal resistance simulation setup and the self-propulsion setup are presented below.

3.1 NOMINAL RESISTANCE SIMULATION SETUP

In order to simulate the LNGC at constant forward speed a Moving Reference Frame (MRF) was applied to the numerical domain. This method allowed running different speeds within one simulation. Opposite to the standard approach of applying an inlet boundary speed, the MRF let to a faster convergence after changing speeds. This is due to the fact that the MRF applies the fluid speed instantly to all cells in the computational domain whereas a change in inlet boundary speed needs to travel from inlet to outlet passing the ship which takes time depending on the inlet speed and the domain length. The STAR-CCM+ Dynamic Fluid Body Interaction (DFBI) module was used to simulate the LNGC in two dimensions of freedom with its motions in response to the fluid forces acting on the ship hull. A mesh dependency study following (Stern et al., 2006) was performed varying the cell size by a factor of $\sqrt{2}$. Refining the mesh in three steps up to around $3\ million$ cells showed a monotonic convergence of the total resistance. The fine-grid convergence index was calculated as

$CGI_{Fine} = 0.07\%$ showing a well converged grid setup. Following (ITTC, 2011) the time step was chosen to be dependent on the ship speed by defining a function $\Delta t = L_{PP}/(v_{Ship} \cdot 200)$ so that the numerical solver finds 200 solutions for a single fluid element traveling along the ship hull. The LNGC performance in nominal resistance conditions was judged by the total resistance and its pressure and shear components (see Figure 7). After convergence was reached a mean value over approximately $10\ sec$ was calculated. The same procedure was followed to calculate the LNGC pitch and heave motions.

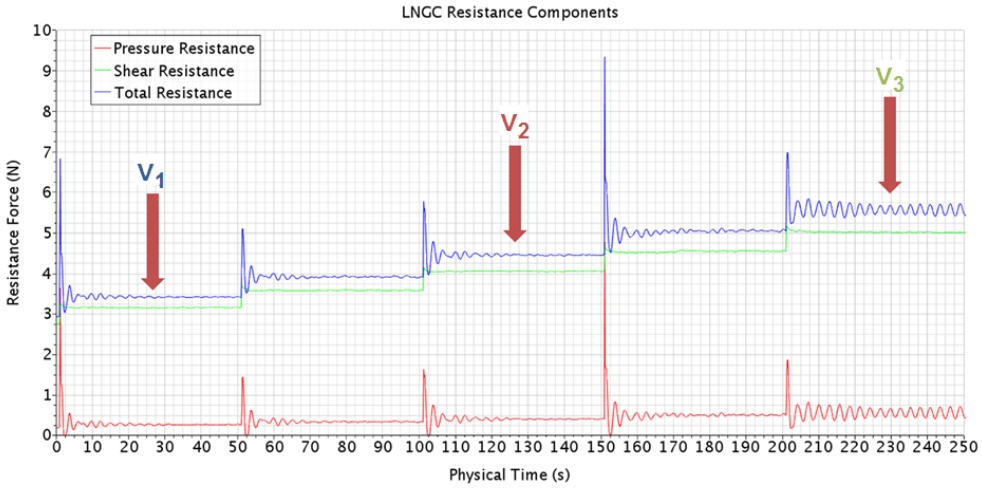

Figure 7 - LNGC resistance monitoring

In addition to the nominal resistance assessment, an indication of how the ship will perform in self-propulsion conditions was also given by comparing the extracted nominal wake fields using a self-developed Wake Analysis Tool (WAT).

3.2 SELF-PROPULSION SIMULATION SETUP

For the self-propulsion simulations the ship geometry was changed to the fully appended LNGC. Additional refinement regions were added around the propeller. The mesh cell size was lowered to properly capture the water-vapour interface defining the cavitation extent. The propeller rotation was simulated using a Sliding Mesh approach. Polyhedral cells were used within the sliding mesh region (see Figure 8) adding around $4.3\ million$ cells to the stationary domain. Similar to the mesh refinement regions, the rotating domain shape was also modelled in CAESES depending on the propeller design.

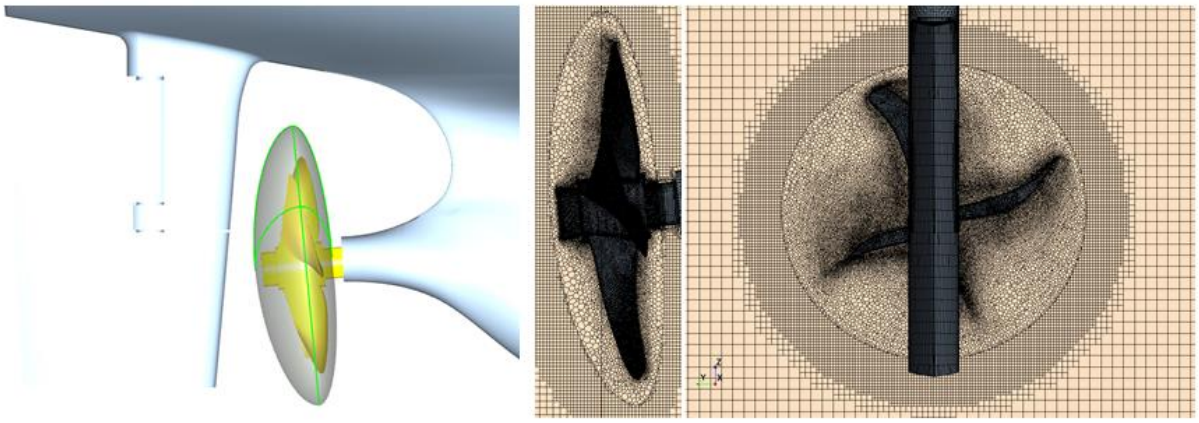

Figure 8 - Polyhedral mesh in the sliding mesh domain around the propeller

The ship was fixed in the domain centre, i.e. no motions were simulated. The initial time step was chosen to be the same as stated above. However, after the flow field converged the time step was reduced so that the thrust and torque generated by the rotating propeller and the cavitation occurrence was captured accurately. With the final self-propulsion time step defined as $\Delta t = 1/(rps \cdot 200)$ the propeller rotated $1.8\ degree$ within one time step. The simulation was initialised with a propeller rotation rate per second of $rps = 0$ which was then smoothly ramped up to an approximate balance between thrust and resistance considering a skin friction correction factor F_0 defined in (ITTC, 2011). After the balance of thrust and resistance was found by manually adjusting the rps, the cavitation model was switched on. The Schnerr-Sauer cavitation model was used throughout all self-

propulsion simulations. Details can be found in (Schnerr and Sauer, 2001).Some simulation time was given to allow the cavitation to initialise and stabilize. Finally the simulation post-processing included the recording of the propeller rps, the delivered power $P_D = 2 \cdot \pi \cdot rps \cdot Q$ (calculated from the propeller torque Q) and the cavitation volume V_{max} in order to judge the propulsive performance.

4. SIMULATION RESULTS

After the simulations converged results were extracted and assessed as described above. The nominal resistance results were evaluated for the LNGC resistance components compared by percentage reduction between level trim and extreme conditions for the three simulated speeds. Furthermore the nominal propeller wake fields were compared visually. For the self-propulsion results rps, delivered power and maximum cavitation volume were compared by percentage reduction.

4.1. NOMINAL RESISTANCE SIMULATION RESULTS

The difference in the floating position between level trim and extreme trim conditions is illustrated in Figure 9. The wave pattern of the level trim simulation shows the developed Kelvin-wake behind the ship, caused by waves leaving the LNGC fore-shoulder and aft-shoulder. The wave pattern of the extreme trim simulation, however, results in a quite unusual wake as the fore-shoulder is not submerged. This indicates that the wave making resistance could be reduced in extreme trim conditions. The side view of the extreme trim case shows that air is sucked below the free surface. It is highly doubted that this is a natural effect of this floating position but a simulation error called numerical ventilation. This might cause the nominal resistance to be under predicted slightly throughout all simulations. This problem could be avoided by solving (instead of modelling) the viscous sub-layer of the boundary flow by using very fine near-wall cells to reach values of $Y+< 1$ (SIEMENS, 2017).

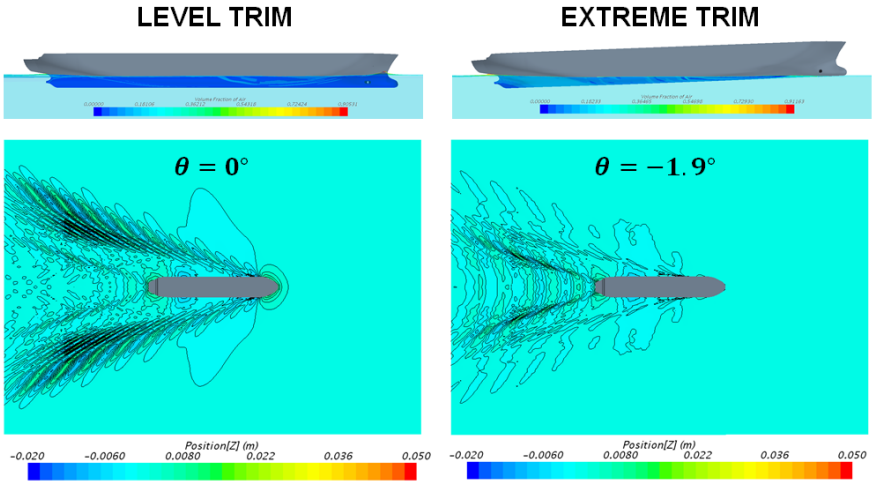

Figure 9 - Side view (top) of the LNGC waterline and top view (bottom) of the LNGC free surface for level and extreme trim for v_3

The comparison of the nominal resistance components (Figure 10) revealed a large force reduction in extreme trim conditions. The largest reduction of total resistance (27.5%) could be found for speed v_3. As already indicated by the wave pattern comparison, the pressure resistance component, related to the wave making resistance, was also largely reduced for all speeds.

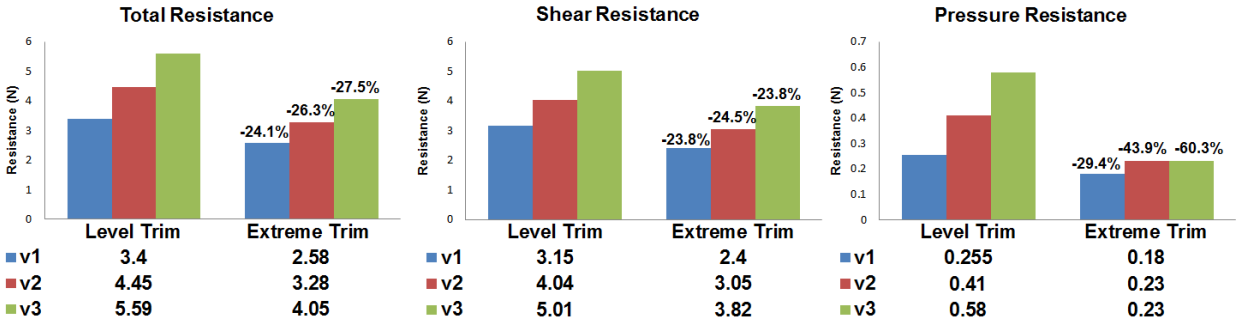

Figure 10 - Nominal resistance components for level trim and extreme trim conditions for three speeds

Dynamic trim and sinkage (i.e. pitch and heave) motions were insignificant for all level trim simulations. The dynamic trim angle was close to zero. For the extreme trim simulations, however, the LNGC dynamically trimmed to stern by a small amount (from $-0.12\ degree$ for v_1 to $-0.17\ degree$ for v_3). This is favourable, as it adds to the propeller tip clearance most likely providing a better self-propulsion performance.

Figure 11 presents the nominal propeller wake fields for each simulation. The level trim wake fields show a clear imprint of the ship located upstream of the propeller plane. This causes the flow velocity to reduce in the upper part of the field forming a so called wake shadow. The extreme trim wake fields show a large area of undisturbed inflow at the bottom. In addition, the wake shadow extent decreased in extreme trim conditions due to a highly reduced blockage of the submerged ship hull.

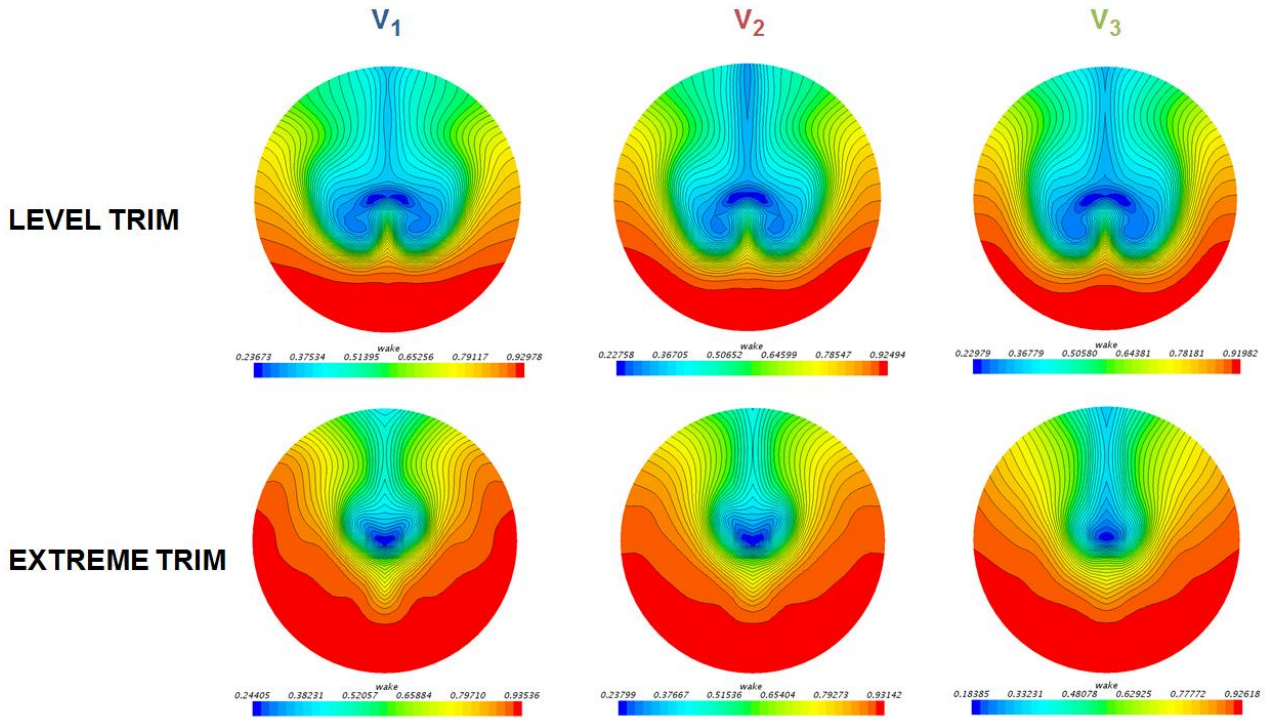

Figure 11 - Nominal wake fields for level trim and extreme trim conditions for three speeds

The numerical analysis of each wake field (Figure 12) revealed that the propeller inflow improves in extreme conditions. The wake uniformity, judged by a reduced axial wake variation and axial wake gradient largely improved for speed v_2. Interestingly, the uniformity parameters increased for speed v_3 indicating an unfavourable propeller inflow and consequently a reduced (lower reduction) self-propulsion performance. The axial mean wake fraction reduced by 50% to around $w \approx 0.2$ for all three speeds. Although the same ship hull is used throughout all simulations, the extreme change of the underwater ship hull (reduction of underwater surface) could be considered as an underwater hull design change. Whereas the LNGC underwater hull form in level trim conditions creates a wake field that would be considered ranking at the lower end of a good propeller inflow, the LNGC in extreme trim conditions represents a rather good design (Tupper, 2004). Due to the increase in inflow homogeneity the cavitation risk is also reduced.

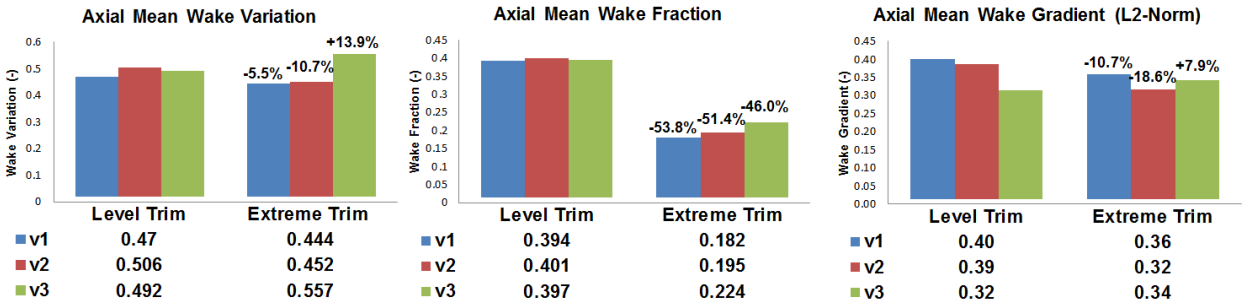

Figure 12 – Numerical analysis (using the WAT) of the nominal wake fields for level trim and extreme trim conditions for three speeds

When summing up the analysis of the resistance components and the nominal wake fields, it is expected that the self-propulsion simulations in extreme trim conditions would predict improvements as a reduced total resistance along with a uniform wake field point at a good self-propulsion performance. Without considering results of the self-propulsion results the combination of resistance reduction and increased wake field homogeneity predicted improvements in self-propulsion conditions for all extreme trim simulations. It was expected that the v_2-simulation would show the best self-propulsion performance.

4.2 SELF-PROPULSION RESULTS

In order to assess the self-propulsion results the same procedure was followed as above. Figure 13 compares the propeller rps, the delivered power P_D and the maximum cavitation volume V_{max} between level trim and extreme trim simulations. Due to the largely reduced LNGC total resistance the propeller rps reduced from level trim to extreme trim by 4.8% for speed v_2. This caused the delivered power to decrease by remarkable 28.8%. The reduction in delivered power for the other two speeds was also high which supports the suggestions made from the nominal resistance simulations results. Worth mentioning is that the v_3-simulation, that showed the largest reduction in total resistance and the nominal wake field with the highest non-uniformity, resulted in the lowest improvement. This indicates that nominal resistance simulations including the assessment of the wake field can predict the ranking of self-propulsion performance quite accurately.

The self-propulsion simulations for speed v_1 did not show any occurrence of cavitation. For the other two speeds the cavitation volume was small and did not have an effect on the thrust and torque. When comparing level trim against extreme trim, the maximum cavitation volume could be reduced by around 40% for both higher speeds. The large reduction of cavitation was not expected as due to the high trim angle the propeller operated in unusual conditions, which was thought to have a negative effect on the development of cavitation. However, because of a decreased rps and a more uniform propeller inflow the propeller seems to work well in extreme trim conditions.

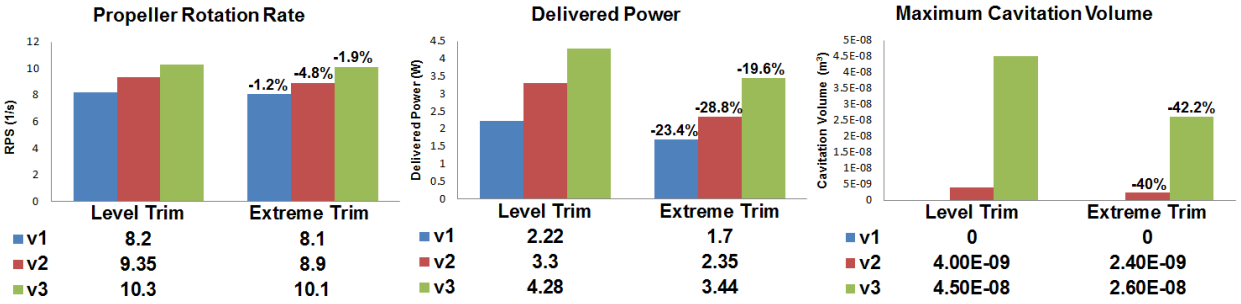

Figure 13 – Self-propulsion performance for level trim and extreme trim conditions for three speeds

The self-propulsion simulations for speed v_1 did not show any occurrence of cavitation. For the other two speeds the cavitation volume was small and did not have an effect on the thrust and torque. Figure 14 shows the cavitation patterns that were typical for level trim and extreme trim simulations. Whereas cavitation appeared on two blades at a time in the wake shadow area, cavitation only occurred on one blade in extreme trim conditions.

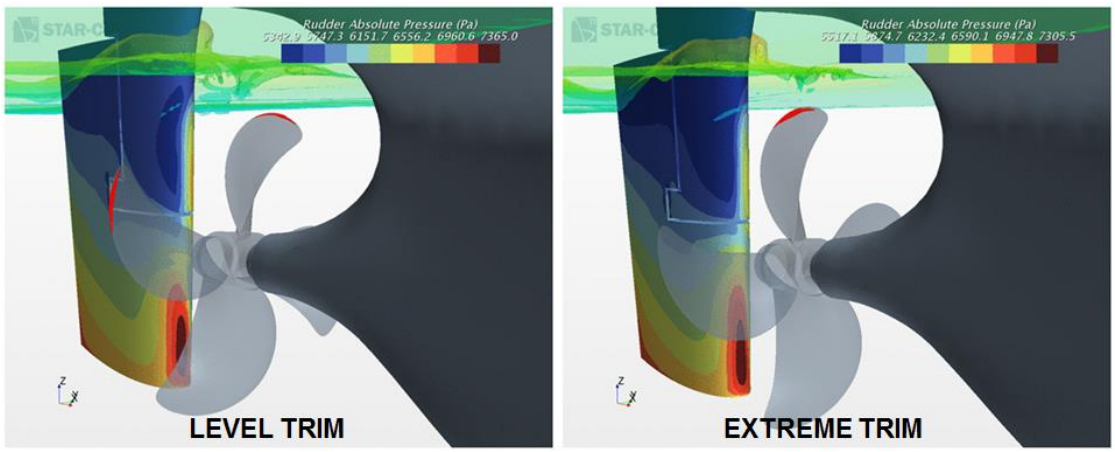

Figure 14 - Cavitation occurrence (iso-value 0.2) for level trim and extreme trim for speed v_3

6. CONCLUSIONS

Considering the large reduction in delivered power (28.8% improvement) predicted by numerical self-propulsion simulations, the extreme trim concept seems to be a promising approach to significantly improve the energy efficiency of an LNG Carrier.

By performing both nominal resistance simulations and self-propulsion simulations including cavitation over a small speed range it could be shown that nominal resistance and the nominal wake field improved significantly. The predicted improvement was validated by the results of the self-propulsion simulations, not only showing a highly improved propulsive performance but also a decrease in cavitation occurrence. Comparing the extreme trim concept to other approaches to significantly improve the energy efficiency of ships, such as moderate trim optimisation, the retrofitting of ship parts (i.e. bulbous bow) or the installation of Energy Saving Devices as outlined in detail by (Mizzi et al., 2015), the presented method seems to be much more efficient. However, the present study only covered a part of necessary calculations to fully predict the performance of a ship under operational conditions. Also, the presented approach is thought to be valid only for ship types similar to an LNGC, therefore the application is limited.

Eventually, it would be advisable to expand the above results by performing additional calculations of the impact of extreme trim on the hull girder and the experimental and numerical prediction of the LNGC performance in waves. In addition, a larger speed range should be covered.

ACKNOWLEDGEMENTS

This research has been funded by the Engineering and Physical Research Council (EPSRC) through the project, “Shipping in Changing Climates. All supports are greatly appreciated. EPSRC grant no. EP/K039253/1. Results were obtained using the EPSRC funded ARCHIE-WeSt High Performance Computer (www.archie-west.ac.uk). EPSRC grant no. EP/K000586/1. The authors would like to further acknowledge Lloyds Register and SHELL as sponsors of this study.

REFERENCES

BIRBANESCU-BIRAN, A. & PULIDO, R. L. 2014. Weight and Trim Calculations. *Ship Hydrostatics and Stability, Second Edition*. 2 ed.: Elsevier Ltd.

GÓRSKI, W., ABRAMOWICZ-GERIGK, T. & BURCIU, Z. 2013. The influence of ship operational parameters on fuel consumption. *Scientific Journals - Zeszyty Naukowe,* 36.

HANSEN, H. & HOCHKIRCH, K. 2013. Lean ECO-Assitant Production for Trim Optimisation. *12th International Conference on Computer and IT Applications in the Maritime Industries.* Cortona: Technische Universitaet Hamburg-Harburg.

ITTC. 2011. ITTC- Recommended Procedures and Guidelines - Practical Guidelines for Ship CFD Applications.

MENTER, F. R. 1994. Two-Equation Eddy-Viscosity Turbulence Models for Engineering Applications. *AIAA Journal,* 32.

MIZZI, K., KIM, M., TURAN, O. & KAKLIS, P. 2015. ISSUES WITH ENERGY SAVING DEVICES AND THE WAY FORWARD *SCC Conference 2015.* Glasgow: University of Strathclyde.

PLOEG, A. V. D. 2012. Object Functions for Optimizing a Ship’s Aft Body. *In:* BERTRAM, V. (ed.) *COMPIT'12 - 11th International Conference on Computer Applications and Information Technology in the Maritime Industries.* Belgium: TUHH Technologie GmbH.

REICHEL, M., MINCHEV, A. & LARSEN, N. L. 2014. Trim Optimisation - Theory and Practice. *20th International Conference on Hydrodynamics in Ship Design and Operation*. Wrocław: FORCE Technology.

SCHNERR, G. H. & SAUER, J. 2001. Physical and Numerical Modeling of Unsteady Cavitation Dynamics. *4th International Conference on Multiphase Flow, New Orleans, USA*.

SIEMENS 2017. STAR-CCM+ Online Documentation. *STEVE PORTAL.*

STERN, F., WILSON, R. & SHAO, J. 2006. Quantitative V&V of CFD simulations and certification of CFD codes. *INTERNATIONAL JOURNAL FOR NUMERICAL METHODS IN FLUIDS*.

TUPPER, E. C. 2004. *Introduction to Naval Architecture*, Elsevier Butterworth-Heinemann.